Neocuproine-Extended Porphyrin Coordination Complexes. 2. Spectroscopic Properties of the Metalloporphyrin Derivatives and Investigations into the HOMO Ordering

Tommaso A. Vannelli and Timothy B. Karpishin*

Department of Chemistry and Biochemistry, University of California, San Diego, La Jolla, California 92093-0358

Received July 30, 1999

The synthesis of a porphyrin compound, **1**, containing a 2,9-dimethyl-1,10-phenanthroline moiety that is fused at the β-pyrrole positions is reported. The absorption spectra of the free-base, copper(II), and zinc(II) derivatives have been studied. On the basis of absorption band intensities, the HOMO of the free base (H_2**1**) and its copper and zinc complexes (Cu**1** and Zn**1**) was determined to be of a_{1u} symmetry. Relative to H_2**1**, compounds Cu**1** and Zn**1** show enhanced spectral changes upon external metal ion binding. Although the HOMO is the same in all three compounds, the energy gap between the two highest occupied orbitals is greater for Cu**1** and Zn**1** than it is for the free-base compound. Several metal ions (Ni^{2+}, Cu^{+}, Cu^{2+}, Zn^{2+}, Li^{+}) were examined in their binding to the phenanthrolinic group by measuring the resulting changes in the absorption spectra. It is shown that the observed changes in the absorption spectra are insensitive to the nature of the metal ion coordinated by the phenanthroline moiety. Significant differences in the absorption and emission spectra between Zn**1** and $[Zn(Zn\mathbf{1})_2]^{2+}$ clearly demonstrate that the porphyrin π-system is strongly affected by the binding of metal ions at the fused phenanthrolinic moiety.

Introduction

Porphyrins have played and continue to play an essential role as building blocks for photoactive molecules and materials, and to model natural photosynthesis. A plethora of methodologies have been employed to couple porphyrin systems to each other and to other molecules of interest such as quinones and carotenoids.[1−10] As multiporphyrin complexes have been extensively examined, numerous electron-transfer and energy-transfer experiments have been undertaken to understand interporphyrin communication in these systems. Desired properties of many systems include enhanced electronic conjugation and/or excitonic communication between the porphyrin units. Recently, Strachan et al. have shown that the nature of the porphyrin highest occupied molecular orbital (HOMO) significantly affects the electron-transfer rates that are observed in various systems.[11] In most porphyrins, there are two high-energy filled MOs, either of which can be the HOMO depending on the porphyrin substituents. A thorough understanding of the orbital structure of the porphyrins is thus germane to one's ability to rationally design and optimize the properties of multiporphyrin systems.

The research presented herein is part of an ongoing pursuit in this laboratory to prepare and examine multiporphyrin complexes assembled via coordination chemistry. Although coordination chemistry has been a method used previously to assemble porphyrin units,[12−20] the majority of systems have utilized a *meso*-pyridyl unit of a *meso*-tetrasubstituted porphyrin as the ligating group. Because of steric interactions, a *meso*-pyridyl group is oriented primarily orthogonal to the porphyrin plane, and is thus somewhat decoupled from the π-system of the porphyrin. The porphyrin building block in our system comprises neocuproine (2,9-dimethyl-1,10-phenanthroline) as the ligating group fused directly to the β-pyrrole carbons of a tetraaryl porphyrin (Figure 1). This design was chosen to maximize the delocalization of π electrons of the porphyrin into

* To whom correspondence should be addressed. Phone: (858) 534-5265. Fax: (858) 534-5383. E-mail: tkarpish@ucsd.edu.

(1) Wasielewski, M. R. *Chem. Rev.* **1992**, *92*, 435−461.
(2) Sessler, J. L.; Capuano, V. L.; Harriman, A. *J. Am. Chem. Soc.* **1993**, *115*, 4618−4628.
(3) Lin, V. S.-Y.; DiMagno, S. G.; Therien, M. J. *Science* **1994**, *264*, 1105−1111.
(4) Harriman, A.; Sauvage, J.-P. *Chem Soc. Rev.* **1996**, 41−48.
(5) Officer, D. L.; Burrell, A. K.; Reid, D. C. W. *Chem. Commun.* **1996**, 1657−1658.
(6) Wagner, R. W.; Johnson, T. E.; Lindsey, J. S. *J. Am. Chem. Soc.* **1996**, *118*, 11166−11180.
(7) Kawabata, S.; Yamazaki, I.; Nishimura, Y.; Osuka, A. *J. Chem. Soc., Perkin Trans. 2* **1997**, 479−484.
(8) Osuka, A.; Shimidzu, H. *Angew. Chem., Int. Ed. Engl.* **1997**, *36*, 135−137.
(9) Jiang, B.; Yang, S.-W.; Barbini, D. C.; Jones, W. E., Jr. *Chem. Commun.* **1998**, 213−214.
(10) Taylor, P. N.; Wylie, A. P.; Huuskonen, J.; Anderson, H. L. *Angew. Chem., Int. Ed.* **1998**, *37*, 986−989.
(11) Strachan, J.-P.; Gentemann, S.; Seth, J.; Kalsbeck, W. A.; Lindsey, J. S.; Holten, D.; Bocian, D. F. *J. Am. Chem. Soc.* **1997**, *119*, 11191−11201.
(12) Crossley, M. J.; Burn, P. L.; Langford, S. J.; Prashar, J. K. *J. Chem. Soc., Chem. Commun.* **1995**, 1921−1923.
(13) Harriman, A.; Odobel, F.; Sauvage, J.-P. *J. Am. Chem. Soc.* **1995**, *117*, 9461−9472.
(14) Hunter, C. A.; Hyde, R. K. *Angew. Chem., Int. Ed. Engl.* **1996**, *35*, 1936−1939.
(15) Allesio, E.; Macchi, M.; Heath, S. L.; Marzilli, L. G. *Inorg. Chem.* **1997**, *36*, 5614−5623.
(16) Flamigni, L.; Armaroli, N.; Barigelletti, F.; Balzani, V.; Collin, J.-P.; Dalbavie, J.-O.; Heitz, V.; Sauvage, J.-P. *J. Phys. Chem. B* **1997**, *101*, 5936−5943.
(17) Linke, M.; Chambron, J.-C.; Heitz, V.; Sauvage, J.-P. *J. Am. Chem. Soc.* **1997**, *119*, 11329−11330.
(18) Amabilino, D. B.; Sauvage, J.-P. *New J. Chem.* **1998**, 395−409.
(19) Drain, C. M.; Nifiatis, F.; Vasenko, A.; Batteas, J. D. *Angew. Chem., Int. Ed.* **1998**, *37*, 2344−2346.
(20) Huck, W. T. S.; Rohrer, A.; Anilkumar, A. T.; Fokkens, R. H.; Nibbering, N. M. M.; vanVeggel, F. C. J. M.; Reinhoudt, D. N. *New J. Chem.* **1998**, 165−168.

10.1021/ic990914q CCC: $19.00
Published on Web 12/30/1999

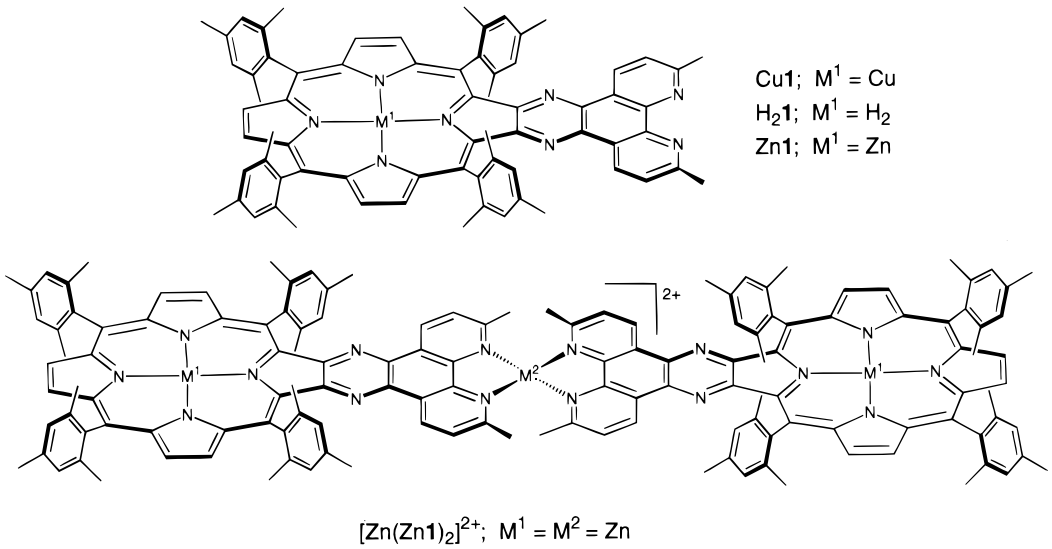

Figure 1. Schematic depiction of the molecules investigated.

the neocuproine unit. Recently reported absorption and emission studies on the free-base molecule, H_2**1**, have shown that there is efficient delocalization of the porphyrin π-system into the neocuproine moiety.[21] This finding led to the investigation of the spectroscopic effects observed upon "external" (i.e., neocuproine) metal ion binding. Upon formation of the zinc(II) and copper(I) complexes of H_2**1**, ($[Zn(H_2\mathbf{1})_2]^{2+}$ and $[Cu(H_2\mathbf{1})_2]^{+}$), significant changes in the emission spectra were observed, as well as changes in the shape and maxima of the absorption bands.[21] These experiments demonstrated that the porphyrin π-system of H_2**1** is sensitive to external metal binding. Thus, metal coordination can be utilized not only to assemble the porphyrin units, but also to control the photophysical properties of the multiporphyrin assemblies.

This work describes investigations of the photophysical properties of the copper(II) and zinc(II) metalloporphyrin derivatives of H_2**1**. As expected, upon "internal" metalation of H_2**1**, there are changes in the absorption and emission spectra of the resultant porphyrins. The spectral effects that are observed upon the binding of metal ions externally to Cu**1** and Zn**1** are dramatically different from the effects that were reported with the free base, H_2**1**. To better understand these differences, the nature of the porphyrin HOMOs in our systems has now been investigated. An effective method that can be used to assign the HOMOs is through analysis of the absorption spectra in a series of molecules.[22,23] Determination of the HOMOs in our molecules allows the photophysical differences observed between Cu**1**/Zn**1** and H_2**1** to be rationalized. Investigation of the external binding of a number of different metal ions has been undertaken to determine if the nature of the external metal ion is important. In addition, the full synthetic procedures used to prepare these novel neocuproine-extended porphyrin complexes are now reported.

Experimental Section

Materials. Chloroform was freshly distilled from K_2CO_3, and the first 10 mL was discarded to remove any ethanol as the $CHCl_3$/ethanol binary azeotrope. Pyrrole was vacuum distilled from CaO immediately prior to use. Methylene chloride used in reactions and for spectroscopy was purified by eluting through a column of Alumina B Super I grade purchased from Selecto Scientific. All NMR solvents were purchased from Cambridge Isotope Laboratories and used without further purification. Acetonitrile used for spectroscopy was UV-grade purchased from Burdick and Jackson. Column chromatography was performed with Silica Gel 60 purchased from EM Science. All other solvents and chemicals were purchased from either Fisher or Aldrich and used without further purification.

Instrumentation. Absorption spectra were collected on a Hewlett-Packard 8452A diode array spectrophotometer. All NMR spectra were obtained on Varian Mercury instruments. Emission spectra were obtained on a Perkin-Elmer LS 50 B luminescence spectrometer.

Titrations. Titrations were performed in acetonitrile. A stock solution of Cu**1** was prepared and its concentration determined spectroscopically using the extinction coefficient at 558 nm. Stock solutions of the metal salts in acetonitrile were prepared, and their concentrations were accurately determined using atomic absorption spectroscopy. The metal solution was then added in 0.1 equiv amounts, and absorption spectra were collected after the mixture was stirred for 2 min. This procedure was continued until 2 equiv had been added. At that point, the metal solution was added in 0.5 equiv amounts up to 4 equiv total.

***meso*-Tetramesitylporphyrin (H_2TMP).** This procedure was adapted from a published protocol[24] that utilizes Lindsey conditions.[25] Under a nitrogen atmosphere with oven-dried glassware, boron trifluoride diethyl etherate (0.244 mL, 1.98 mmol) was added to a rapidly stirring solution of mesitaldehyde (4.0 mL, 27.1 mmol) and pyrrole (1.9 mL, 6.01 mmol) in $CHCl_3$ (500 mL). The reaction flask was covered in aluminum foil and stirred at room temperature for 1 h. Triethylamine (0.334 mL, 2.40 mmol) was added followed by 2,3-dichloro-5,6-dicyano-1,4-benzoquinone (1.026 g, 4.52 mmol). The resultant mixture was then heated at reflux for 1 h. The crude reaction mixture was evaporated to dryness, and the solid residue was triturated with diethyl ether. The ether was evaporated, the solid was dissolved in a minimal amount of CH_2Cl_2, and the mixture was purified on silica (eluent CH_2Cl_2). The leading dark red band was collected. This fraction was evaporated to dryness, resulting in 441 mg (0.563 mmol) of H_2TMP as a purple microcrystalline solid (38% yield). UV−vis [λ_{max} (nm) (log(ϵ), M^{-1} cm^{-1})]: CH_2Cl_2, 418 (5.63), 514 (4.25), 546 (3.74), 590 (3.72), 646 (3.45). ^{1}H NMR ($CDCl_3$, 400 MHz) [δ (ppm)]: −2.53 (2H, s, N**H),** 1.83 (24H, s, *o*-aryl-C-**H$_3$**), 2.60 (12H, s, *p*-aryl-C**H$_3$**), 7.25 (8H, s, *m*-aryl-**H**), 8.60 (8H, s, pyrrole-β-**H**).

***meso*-Tetramesitylporphyrinatozinc(II) (ZnTMP).** A saturated methanolic solution of $Zn(CH_3CO_2)_2 \cdot 2H_2O$ (1 mL) was added to a refluxing solution of H_2TMP (30 mg, 0.038 mmol) in 30 mL of $CHCl_3$.

(21) Vannelli, T. A.; Karpishin, T. B. *Inorg. Chem.* **1999**, *38*, 2246−2247.
(22) Spellane, P. J.; Gouterman, M.; Antipas, A.; Kim, S.; Liu, Y. C. *Inorg. Chem.* **1980**, *19*, 386−391.
(23) Binstead, R. A.; Crossley, M. J.; Hush, N. S. *Inorg. Chem.* **1991**, *30*, 1259−1264.
(24) Bookser, B. C.; Bruice, T. C. *J. Am. Chem. Soc.* **1991**, *113*, 4208−4218.
(25) Lindsey, J. S.; Wagner, R. W. *J. Org. Chem.* **1989**, *54*, 828.

The reaction was monitored by absorption spectroscopy and silica TLC (eluent 50% CH_2Cl_2, 50% hexanes). Total conversion to the desired product was observed after 5 min. The solution was cooled to room temperature, poured over a silica gel plug, and eluted with 1 L of CH_2Cl_2. After evaporation of the solvent, 30 mg (0.035 mmol) of a pink/purple solid was obtained (92% yield). UV−vis [λ_{max} (nm)]: CH_2Cl_2, 420, 512, 550, 586.

***meso*-Tetramesitylporphyrinatocopper(II) (CuTMP).** The free-base porphyrin (H_2TMP) (0.738 g, 1.28 mmol) was dissolved in 400 mL of $CHCl_3$, and the solution was brought to reflux. To this solution was added 35 mL of a solution of $Cu(CH_3CO_2)_2 \cdot H_2O$ (0.750 g, 3.76 mmol) in CH_3OH. The reaction was monitored by absorption spectroscopy and silica TLC (eluent 50% CH_2Cl_2, 50% hexanes). Total conversion to the desired product was observed after 10 min. The solution was cooled to room temperature, poured over a silica gel plug, and eluted with 1 L of $CHCl_3$. After evaporation of the solvent, 985 mg (1.17 mmol) of a red solid was obtained (91% yield). UV−vis [λ_{max} (nm)]: CH_2Cl_2, 416, 540, 574.

2-Nitro-*meso*-tetramesitylporphyrinatocopper(II) (CuTMP-β-NO_2). This procedure was based upon a literature protocol.[26] The copper porphyrin (CuTMP) (147 mg, 0.174 mmol) was dissolved in 30 mL of CH_2Cl_2 in a 250 mL round-bottom flask equipped with a stir bar and sealed with a rubber septum. NO_2(g) (8.8 mL, 0.36 mmol; calculated using the ideal gas law) was added in two portions using a conventional plastic syringe. The reaction was monitored with silica TLC (eluent 60% hexanes, 40% CH_2Cl_2). After the mixture was stirred for 30 min, with the appearance of dinitrated products, the reaction was terminated by flushing with nitrogen. Chromatographic purification was accomplished by preadsorbing the dissolved product on a minimal amount of silica and loading this dried powder on a silica column (22 × 5 cm; l × d) packed with hexanes. The material was eluted with a gradient of CH_2Cl_2 (2−50%; 2% per 200 mL). The starting material (CuTMP) eluted first (25−30% CH_2Cl_2) followed by the desired mononitrated product (38−44% CH_2Cl_2). This procedure yielded 151 mg (0.17 mmol) of the desired product (98% yield). UV−vis [λ_{max} (nm)]: CH_2Cl_2, 420, 546, 584. MALDI MS: obsd *m*/*z* 891 $(M + H)^+$, calcd for $C_{56}H_{51}N_5O_2Cu$ 890.

2-Amino-*meso*-tetramesitylporphyrinatocopper(II) (CuTMP-β-NH_2). This procedure was based upon a literature protocol.[27] Rigorously anaerobic techniques were employed, and all glassware was oven dried and cooled under a nitrogen flow. A round-bottom side arm flask was charged with 127 mg (0.143 mmol) of CuTMP-β-NO_2. The material was subsequently dissolved in 30 mL of dry CH_2Cl_2 and 10 mL of dry CH_3OH. Palladium (10% on carbon) catalyst (120 mg) was added and the solution purged with N_2 for 5 min. Sodium borohydride (130 mg, 3.43 mmol) was added to the solution in portions over 10 min. The reaction mixture was tested by silica TLC (eluent 60% hexanes, 40% CH_2Cl_2) until all starting material (CuTMP-β-NO_2) was consumed. The amino product appears as a brown/red spot that turns green over time on the plate, while CuTMP-β-NO_2 is a stable red spot that moves slightly faster than the amino product. Although the reaction appeared complete after 45 min, it was stirred overnight under N_2 in the dark. The mixture was then cannula filtered into a dry round-bottom flask. The solution was evaporated to dryness and the solid residue extracted with dry CH_2Cl_2 until the solution was clear. The extraction was performed using two cannulas, one to deliver the CH_2Cl_2 and one to filter off the solution, leaving the insoluble material behind. The solvent was then evaporated, and the air-sensitive product was carried on to the next reaction without further purification.

2,3-Dioxo-*meso*-tetramesitylchlorinatocopper(II) ($CuTMCO_2$). This procedure was based upon a literature protocol.[28] The amino derivative (CuTMP-β-NH_2) was dissolved in 20 mL of dry CH_2Cl_2, and the solution was purged with dry O_2 for 2 min. The flask was sealed with a septum and irradiated with ambient sunlight. The solution turned green after approximately 5 min. The reaction was monitored by silica TLC (eluent 50% CH_2Cl_2, 50% hexanes). A green spot due to the product appeared that moved slower than CuTMP-β-NH_2. The solution was allowed to stir for 2 days in the window sill and purged twice daily with dry O_2. When no further reaction was observable by TLC, the solvent was evaporated and the solid residue purified by flash column chromatography. A silica column (22 × 5 cm; l × d) was packed with a solution of 75% hexanes and 25% CH_2Cl_2. The column was then eluted with a gradient of CH_2Cl_2 (25−70%; 5% per 200 mL). This purification resulted in 69 mg (0.079 mmol) of the desired product (55% yield based on CuTMP-β-NO_2 used). UV−vis [λ_{max} (nm)]: CH_2Cl_2, 408, 490. FAB MS: obsd *m*/*z* 875 $(M + H)^+$, 1006 $(M + Cs)^+$, calcd for $C_{56}H_{50}N_4O_2Cu$ 874.

2,9-Dimethyl-5-nitro-1,10-phenanthroline (NO_2nc). This procedure was adapted from a previously published preparation of 5-nitro-1,10-phenanthroline.[29] Neocuproine (1.000 g, 4.419 mmol) was dissolved in 5 mL of oleum (100 mmol), and concentrated HNO_3 (2.67 mL, 43 mmol) was added dropwise so that the solution temperature never exceeded 170 °C. The solution was placed in an oil bath at 160 °C for 30 min. The reaction mixture was cooled to room temperature, poured over 70 g of ice, and neutralized with 0.6 M aqueous NaOH (400 mL). Enough concentrated HNO_3 was then added to make the solution slightly acidic (pH ≈ 5−6). Precipitation occurred overnight, after which the solid was filtered. The filtrate was then further acidified with concentrated HNO_3 (pH ≈ 4), allowed to sit overnight, and filtered. The solids were combined, yielding 544 mg (2.15 mmol) of pure product (49% yield). ^{1}H NMR (CD_3OD, 300 MHz) [δ (ppm)]: 2.90 (3H, s, C**H**$_3$), 2.91 (3H, s, C**H**$_3$), 7.73 (1H, d, 8-**H**, J = 8.0 Hz), 7.76 (1H, d, 3-**H**, J = 8.8 Hz), 8.46 (1H, d, 7-**H**, J = 8.0 Hz), 8.71 (1H, s, 6-**H**), 8.84 (1H, d, 4-**H**, J = 8.8 Hz). FAB MS: obsd *m*/*z* 254 $(M + H)^+$ and 276 $(M + Na)^+$, calcd for $C_{14}H_{11}N_3O_2$ 253.

6-Amino-2,9-dimethyl-5-nitro-1,10-phenanthroline (NO_2NH_2nc). This procedure was based upon a literature protocol.[30] Hydroxylamine hydrochloride (1.458 g, 20.98 mmol) was added to a suspension of NO_2nc (0.759 g, 3.00 mmol) in 16.8 mL of absolute ethanol. The mixture was brought to reflux, and 17 mL of an ethanolic KOH (1.66 M) solution was added dropwise over 25 min. After 40 min, the reaction mixture was cooled to room temperature and poured into 20 mL of ice cold water. The mixture was filtered (Whatman 50) and washed with water, ethanol, and $CHCl_3$, affording 227 mg of pure product. Recrystallization of the material in the filtrate from ethanol and brine resulted in an additional 89 mg of product. The final yield of this reaction was 39% (316 mg, 1.18 mmol). ^{1}H NMR (d_6-DMSO, 300 MHz) [δ (ppm)]: 2.66 (3H, s, C**H**$_3$), 2.77 (3H, s, C**H**$_3$), 7.52 (1H, d, 8-**H**, J = 8.4 Hz), 7.70 (1H, d, 3-**H**, J = 8.7 Hz), 8.57 (2H, br s, N**H**$_2$), 8.66 (1H, d, 7-**H**, J = 8.4 Hz), 8.91 (1H, d, 4-**H**, J = 8.7 Hz).

5,6-Diamino-2,9-dimethyl-1,10-phenanthroline (danc). This procedure was based upon a literature protocol.[30] Under a nitrogen atmosphere with oven-dried glassware, neat hydrazine monohydrate (743.6 μL, 15.33 mmol) was added dropwise to a refluxing ethanol (176 mL) solution of NO_2NH_2nc (196 mg, 0.731 mmol) and Pd on activated carbon (5%, 198 mg). After 1 h of heating at reflux, the solution was filtered hot (Whatman 50). The volume of the filtrate was reduced by 50%, an equal volume of acetone added, and the solution stored at 6 °C overnight. Filtration of this solution resulted in 51 mg (0.214 mmol, 29% yield) of the desired product. ^{1}H NMR (d_6-DMSO, 300 MHz) [δ (ppm)]: 2.68 (6H, s, C**H**$_3$), 5.04 (4H, br s, N**H**$_2$), 7.44 (2H, d, 3,8-**H**, J = 8.5 Hz), 8.33 (2H, d, 4,7-**H**, J = 8.5 Hz).

(2′,9′-Dimethylpyrazo[5′,6′-*e*]-1′,10′-phenanthroline)[*b*]-*meso*-tetramesitylporphyrinatocopper(II) (Cu1). This procedure was based upon a literature protocol.[31] Under a nitrogen atmosphere with oven-dried glassware, a catalytic amount of trifluoroacetic acid (50 μL, 650 μmol) was added to a solution of danc (62 mg, 0.26 mmol) and $CuTMCO_2$ (69 mg, 79 μmol) in 150 mL of dry CH_2Cl_2 at reflux. Silica TLC (eluent 5% MeOH in CH_2Cl_2) analysis after 10 min showed that

(26) Catalano, M. M.; Crossley, M. J.; Harding, M. M.; King, L. G. *J. Chem. Soc., Chem. Commun.* **1984**, 1535−1536.
(27) Baldwin, J. E.; Crossley, M. J.; DeBernardis, J. *Tetrahedron* **1982**, *38*, 685−692.
(28) Crossley, M. J.; King, L. G. *J. Chem. Soc., Chem. Commun.* **1984**, 920−922.
(29) Smith, G. F.; Cagle, F. W., Jr. *J. Org. Chem.* **1947**, *12*, 781−784.
(30) Bolger, J.; Gourdon, A.; Ishow, E.; Launay, J.-P. *Inorg. Chem.* **1996**, *35*, 2937−2944.
(31) Kozyrev, A. N.; Alderfer, J. L.; Srikrishnan, T.; Pandey, R. K. *J. Chem. Soc., Perkin Trans. 1* **1998**, 837−838.

the reaction was approximately 50% complete. The mixture was shielded from light and heated at reflux overnight. After being cooled to room temperature, the mixture was stirred over an equal volume of 4% aqueous sodium bicarbonate, washed with water (2 × 150 mL) and brine (75 mL), and dried over Na_2SO_4. The solution was then loaded onto a silica column (12 × 6 cm; l × d) packed in CH_2Cl_2. The desired product was eluted with a gradient of CH_3OH (1/2% per 50 mL) up to 4%, at which point the product eluted off the column with 400 mL of 4% MeOH. This method afforded 80 mg (74 μmol) of pure material as a purple/brown solid (94% yield). UV−vis [λ_{max} (nm) (log(ϵ), M^{-1} cm^{-1})]: MeCN, 404 (4.97), 442 (5.09), 524, 558 (4.27), 598 (3.92). ESI MS: obsd *m*/*z* 1076.5 $(MH)^+$, calcd for $C_{70}H_{60}N_8Cu$ 1075.5.

(2′,9′-Dimethylpyrazo[5′,6′-*e*]-1′,10′-phenanthroline)[*b*]-*meso*-tetramesitylporphyrin ($H_2$1). This procedure was based upon a literature protocol.[32] Concentrated sulfuric acid (62 μL, 1.12 mmol) was added slowly to a rapidly stirring solution of Cu**1** (15 mg, 0.014 mmol) in 5 mL of CH_2Cl_2. The flask was shielded from light and the solution stirred for 5 min, at which time all the porphyrin material had dissolved in the acid layer. The mixture was then stirred over an equal volume of aqueous EDTA (0.01 M H_4EDTA, 0.1 M acetate buffer, pH 4.7). The organic layer was separated, and the aqueous layer was further washed with CH_2Cl_2 until the organic washes were clear. The combined CH_2Cl_2 solutions were washed with equal volumes of 4% aqueous sodium bicarbonate, water, and brine. The solution was dried with Na_2SO_4 and the solvent evaporated. The reaction proceeded quantitatively, yielding 14 mg (0.014 mmol) of pure H_2**1**. UV−vis [λ_{max} (nm) (log(ϵ), M^{-1} cm^{-1})]: CH_2Cl_2, 438 (5.04), 526 (4.00), 562 (sh), 598 (3.70), 654. ^{1}H NMR ($CDCl_3$, 400 MHz) [δ (ppm)]: −2.40 (2H, br s, N**H**), 1.81 (12H, s, *o*-aryl-C-**H$_3$**), 1.89 (12H, s, *o*-aryl-C**H$_3$**), 2.63 (6H, s, *p*-aryl-C**H$_3$**), 2.87 (6H, s, *p*-aryl-C**H$_3$**), 3.04 (6H 2,9-phenanthroline-C**H$_3$**), 7.28 (4H, s, *m*-aryl-**H**), 7.45 (4H, s, *m*-aryl-**H**), 7.64 (2H, d, 3,8-phenanthroline-**H**, J = 8.4 Hz), 8.55 (2H, s, pyrrole-β-**H**), 8.78 (2H, d, pyrrole-β-**H**, J = 5.1 Hz), 8.87 (2H, d, pyrrole-β-**H**, J = 5.1 Hz), 8.92 (2H, d, 4,7-phenanthroline-**H**, J = 8.4 Hz). FAB MS: obsd *m*/*z* 1015 $(MH)^+$ and 1147 $(M + Cs)^+$, calcd for $C_{70}H_{62}N_8$ 1014.

(2′,9′-Dimethylpyrazo[5′,6′-*e*]-1′,10′-phenanthroline)[*b*]-*meso*-tetramesitylporphyrinatozinc(II) (Zn1). A saturated methanolic solution of $Zn(CH_3CO_2)_2 \cdot 2H_2O$ (1 mL) was added to a solution of H_2**1** (14 mg, 14 μmol) in 25 mL of $CHCl_3$ at reflux. The reaction was heated overnight, after which UV/vis analysis of the Q bands showed complete conversion to the metalated porphyrin. The cooled solution was then stirred with an equal volume of aqueous EDTA (0.01 M H_4EDTA, 0.1 M acetate buffer, pH 4.7) for 24 h. The organic layer was separated and washed with 50 mL each of 4% aqueous sodium bicarbonate, water, and brine. The material was then purified using silica chromatography with $CHCl_3$ as the eluent (6.5 × 6.5 cm; l × d). This method yielded 10.6 mg (9.8 μmol, 71%) of the desired product in high purity. UV−vis [λ_{max} (nm) (log(ϵ), M^{-1} cm^{-1})]: MeCN, 446 (4.7), 538 (3.8), 576 (4.3), 616 (3.8). ^{1}H NMR ($CDCl_3$, 400 MHz) [δ (ppm)]: 1.81 (12H, s, *o*-aryl-C-**H$_3$**), 1.88 (12H, s, *o*-aryl-C**H$_3$**), 2.62 (6H, s, *p*-aryl-C**H$_3$**), 2.87 (6H, s, *p*-aryl-C**H$_3$**), 3.02 (6H 2,9-phenanthroline-C**H$_3$**), 7.28 (4H, s, *m*-aryl-**H**), 7.45 (4H, s, *m*-aryl-**H**), 7.65 (2H, d, 3,8-phenanthroline-**H**, J = 8.0 Hz), 8.65 (2H, s, pyrrole-β-**H**), 8.76 (2H, d, pyrrole-β-**H**, J = 4.8 Hz), 8.82 (2H, d, pyrrole-β-**H**, J = 4.8 Hz), 8.96 (2H, d, 4,7-phenanthroline-**H**, J = 8.0 Hz). ESI MS: obsd *m*/*z* 1077 $(MH)^+$, calcd for $C_{70}H_{60}N_8Zn$ 1076.

[Zn(Zn1)$_2$](CH$_3$CO$_2$)$_2$. A methanolic saturated solution of $Zn(CH_3CO_2)_2 \cdot 2H_2O$ (0.5 mL) was added to a nitrogen-purged solution of Zn**1** (5.3 mg, 4.9 μmol) in 10 mL of $CHCl_3$. The mixture was shielded from light and stirred for 5 min under a nitrogen atmosphere. The solvent was evaporated, and the solid residue was taken up in a minimal amount of CH_2Cl_2 and filtered through Celite 521. The reaction proceeds quantitatively. UV−vis [λ_{max} (nm)]: CH_2Cl_2, 418, 456, 538, 576, 614. ^{1}H NMR ($CDCl_3$, 300 MHz) [δ (ppm)]: 1.78 (12H, s, *o*-aryl-C-**H$_3$**), 1.87 (12H, s, *o*-aryl-C**H$_3$**), 2.01 (6H, CO_2C**H$_3$**), 2.62 (6H, s, *p*-aryl-C**H$_3$**), 2.85 (6H, s, *p*-aryl-C**H$_3$**), 3.26 (6H 2,9-phenanthroline-C**H$_3$**), 7.27 (4H, s, *m*-aryl-**H**), 7.43 (4H, s, *m*-aryl-**H**), 7.85 (2H, d, 3,8-phenanthroline-**H**, J = 8.4 Hz), 8.66 (2H, s, pyrrole-β-**H**), 8.76 (2H, d, pyrrole-β-**H**, J = 4.8 Hz), 8.83 (2H, d, pyrrole-β-**H**, J = 4.8 Hz), 9.13 (2H, d, 4,7-phenanthroline-**H**, J = 8.4 Hz). MALDI MS: obsd *m*/*z* 2217$(M + e^-)^+$, calcd for $C_{140}H_{120}N_{16}Zn_3$ 2217.

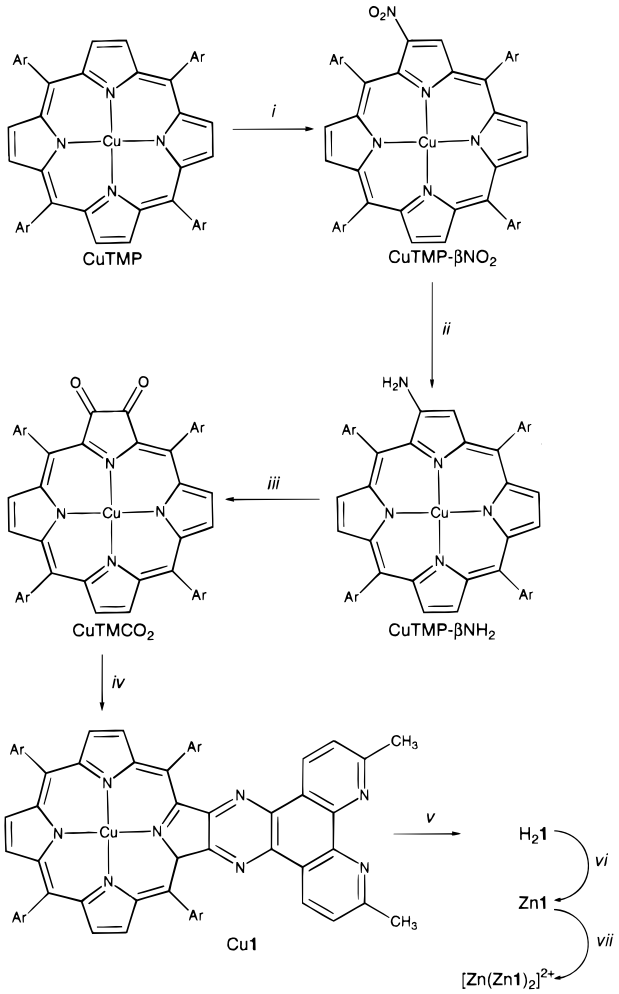

Figure 2. Synthetic scheme for the preparation of the molecules investigated. Ar = 2,4,6-trimethylphenyl. Conditions: (i) 2 equiv of NO_2 in dry CH_2Cl_2; (ii) Pd/C, $NaBH_4$ in CH_2Cl_2/MeOH; (iii) O_2/$h\nu$ in dry CH_2Cl_2; (iv) 3.3 equiv of danc, 0.033% TFA in CH_2Cl_2; (v) CH_2Cl_2/H_2SO_4; (vi) $Zn(CH_3CO_2)_2$ in $CHCl_3$/EDTA; (vii) $Zn(CH_3CO_2)_2$ in $CHCl_3$.

Results and Discussion

(I) Syntheses. Figure 2 presents the synthetic strategy used to obtain compounds H_2**1**, Cu**1**, and Zn**1**. Reaction of the copper(II) porphyrin (CuTMP) with NO_2 is essential for a clean reaction to the nitrated complex (CuTMP-β-NO_2) because the regiospecificity of the nitration is directed by the electronegativity of the central metal ion.[26] If one nitrates a zinc or free-base tetraarylporphyrin, oxidation occurs at the *meso* positions and the porphyrin ring is ruptured.[26] Reaction of CuTMP with NO_2 usually produced a small amount of dinitrated products which were easily removed by column chromatography. Care must be taken to not add too much NO_2 and to not let the reaction proceed for too long, since such conditions favor the formation of polynitrated species. Silica TLC analysis was found to be an effective means by which this reaction could be monitored.

Reduction of CuTMP-β-NO_2 proceeds smoothly, but must be performed under rigorously maintained inert atmosphere conditions. The amino derivative (CuTMP-β-NH_2) is extremely

(32) Beavington, R.; Rees, P.; Burn, P. *J. Chem. Soc., Perkin Trans. 1* **1998**, 2847−2851.

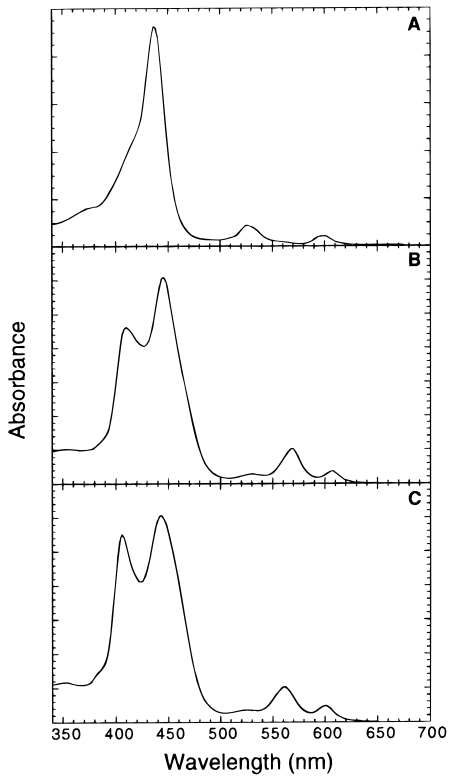

Figure 3. Absorption spectra in CH_2Cl_2 at room temperature of H_2**1** (A), Zn**1** (B), and Cu**1** (C).

reactive to hydrolysis and must be handled with care.[27] Once CuTMP-β-NH_2 is oxidized to the dioxochlorin, $CuTMCO_2$, these precautions are no longer necessary since $CuTMCO_2$ is air stable. The dioxochlorin is then subjected to a condensation with 5,6-diaminoneocuproine (danc, Figure 2). The synthesis of danc was carried out in a manner similar to that reported for the preparation of 5,6-diamino-1,10-phenanthroline.[30] However, the yield (29%) in the final step of the synthesis of danc fell well below the reported yield for the analogous reaction performed with 1,10-phenanthroline (83%).[30]

The conditions used for the condensation of $CuTMCO_2$ with danc were based upon the reported work of Pandey et al.[31] These conditions were found to be far superior to conditions reported by Crossley et al. for a similar condensation.[12] The condensation reaction produces the desired product (Cu**1**) in high yield (94%). Demetalation of Cu**1** with H_2SO_4 generates H_2**1**, which is then metalated with zinc(II) acetate to provide Zn**1**. Although Cu**1** is indefinitely stable, the free base (H_2**1**) and zinc(II) complex (Zn**1**) are susceptible to photooxidation if exposed to light in solution for extended periods of time. We have also observed that the copper(I) and zinc(II) complexes of H_2**1**, $[Cu(H_2\mathbf{1})_2]^+$, and $[Zn(H_2\mathbf{1})_2]^{2+}$ slowly undergo transmetalation, whereby the externally coordinated metal is transferred to the porphyrin core. This process occurs overnight in solution and over a period of a couple of months in the solid state. Transmetalation is not a problem with the metal complexes of the metallo derivatives (Cu**1** and Zn**1**).

(II) Absorption Spectra. (a) General Features. The spectral features of H_2**1** have been previously reported.[21] The absorption spectra of H_2**1**, Cu**1**, and Zn**1** are shown in Figure 3. They are typical porphyrin spectra in that they contain a strong absorption band in the UV region, designated as the B band, and weaker visible absorption bands designated as the Q bands. The copper porphyrin, Cu**1**, displays a *hypso* type spectrum which is in accord with the fact that it is an irregular porphyrin, while the zinc porphyrin, Zn**1**, being a regular porphyrin, displays a normal type spectrum.[33] The Q-band envelope of both Cu**1** and Zn**1** contains the Q(0,0) transition as well as the two vibronic overtones, Q(1,0) and Q(2,0) (Table 1). These are typical characteristics common to all metalloporphyrins.

Table 1. Absorption Maxima and Band Assignments[a]

	B(0,0)	Q(2,0)	Q(1,0)	Q(0,0)
Cu**1**	406 (B_y), 442 (B_x)	526	560	600
H_2**1**	438		526 (Q_y), 598 (Q_x)	562 (Q_y), 654 (Q_x)
Zn**1**	412 (B_y), 446 (B_x)	532	568	608

[a] All values are reported in nanometers, and the spectra were performed in CH_2Cl_2 at room temperature.

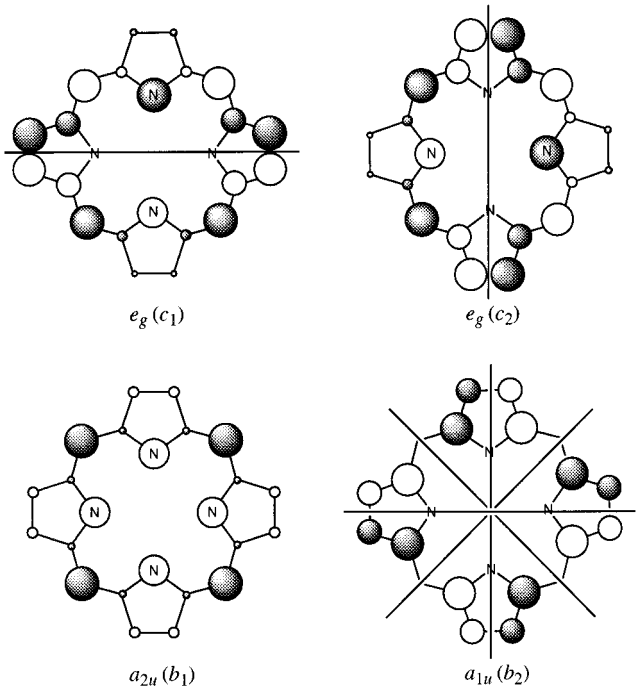

Figure 4. Representation of the electron densities in the two HOMOs (bottom) and the two LUMOs (top) for the D_{4h} porphyrin ring.[23]

(b) Theory. Gouterman's early research resulted in the widely accepted four-orbital porphyrin model which is a combination of simple Hückel calculations with the free-electron and cyclic polyene models.[33,34] This theory proposes that all porphyrin systems contain two nearly degenerate top-filled π orbitals and two lowest unoccupied molecular orbitals (LUMOs) that are degenerate. In the case of perfect D_{4h} symmetry, the top-filled orbitals differ in their nodal and density structure, resulting in an orbital of a_{2u} symmetry and one having a_{1u} symmetry (Figure 4). On the other hand, the two LUMOs both have e_g symmetry. Since the porphyrin molecules discussed in this paper have C_{2v} symmetry rather than D_{4h} symmetry, we will refer to the a_{2u} and a_{1u} orbitals as b_1 and b_2, respectively, and the two e_g orbitals as c_1 and c_2 (Figure 4). Gouterman's model adequately explains the electronic absorption spectra of most porphyrinic compounds and thus is the foundation for many orbital-based explanations of the electronic properties of porphyrin-containing complexes.

A knowledge of the relative energy levels of these four orbitals in the individual porphyrins within a multiporphyrin system is relevant to understanding interporphyrin ground-state and excited-state electronic communication. If one wishes to

(33) Gouterman, M. *The Porphyrins*; Academic Press: New York, 1978; Vol. III.
(34) Gouterman, M. *J. Mol. Spectrosc.* **1961**, *6*, 138−163.

Table 2. A(Q(0,0))/A(Q(1,0)) Values for Selected Compounds

	PFP[a]	TPP[a]	TMP	**1**
H_2[b]	0.13	0.43	0.39	0.30
Zn	0.26	0.13	0.11	0.43
Cu	0.47	0.095	0.093	0.45
Cu-β-NO_2		0.65	0.42	

[a] Taken from ref 22. [b] For the free-base compounds the ratio of the sums of the x and y components of the Q transitions was used $[A(Q_x(0,0)) + A(Q_y(0,0))]/[A(Q_x(1,0)) + A(Q_y(1,0))]$.

link the chromophores via the *meso* position, then a porphyrin with the b_1 orbital as the HOMO is desirable to maximize electronic coupling. On the other hand, if one wishes to join the chromophores through the β-pyrrole positions, then a porphyrin with a b_2 HOMO is desirable. Inspection of the two top-filled orbitals in Figure 4 shows that the b_1 orbital is stabilized either by electron-withdrawing groups at the *meso* positions or by metal ion coordination by the pyrrole nitrogens. The b_2 orbital can be stabilized only by electron-withdrawing groups on the β-pyrrole carbons.

Coupling between the four electronic transitions from the two top-filled orbitals into the two LUMOs results in the high-energy B state and the low-energy Q state observed in porphyrin absorption and emission spectra.[33] The two pairs of singlet transitions in which these orbitals are involved are $a_{2u} \rightarrow e_g$ and $a_{1u} \rightarrow e_g$. According to the four-orbital model, when the top-filled π orbitals are equal in energy and the two unoccupied π^* orbitals are also equal in energy, the B and Q states are comprised of two degenerate transitions polarized in the x and y directions.[33] In this case the Q state is formally forbidden.[33] If this degeneracy is lifted, then the Q(0,0) transition becomes partially allowed.[33,34] Therefore, the intensity of the Q(0,0) absorption band is directly related to the energy spacing between the two HOMOs. The degree of degeneracy and the energy splitting of the two top-filled π orbitals can be determined through analysis of the absorption spectra in the low-energy region (the Q-band region).[22,23] This method utilizes the intensity ratio of the two visible transitions typical of porphyrin absorption spectra. The two transitions used are Q(0,0) and its vibronic overtone Q(1,0). The Q(1,0) transition arises from vibronic mixing of the Q state with the B state, and its intensity varies little among various porphyrins.[22,33] The intensity of the Q(1,0) transition can, thus, be used as a normalizing factor when different porphyrin compounds are compared. This ratio is related to the energy of the HOMO by the following equation:

$$A[\mathrm{Q}(0,0)]/A[\mathrm{Q}(1,0)] = (\mathrm{const})[^1E(a_{2u},e_g) - {}^1E(a_{1u},e_g)]^2 \quad (1)$$

where $^1E(a_{2u},e_g) - {}^1E(a_{1u},e_g)$ is the energy gap between the two pairs of singlet transitions.

(c) Nature of the HOMOs. Q-Band Analysis of $H_2$1, Cu1, and Zn1. Here we compare the experimentally determined Q-band ratios for our compounds with those of other benchmark porphyrins such as *meso*-tetraphenylporphyrin, TPP, and its tetra(pentafluorophenyl) analogue, PFP. Using the ratios in Table 2 we can then plot $\{A[\mathrm{Q}(0,0)]/A[\mathrm{Q}(1,0)]\}^{1/2}$, which in turn can be used to determine which of the two top-filled porphyrin orbitals is the HOMO. This plot is shown in Figure 5.

The compounds H_2TMP, CuTMP, CuTMP-β-NO_2, and ZnTMP are spectroscopically very similar to their TPP analogues, which is reflected in the fact that they all have a HOMO that is a_{2u} (b_1) in character. This is not surprising since the mesityl groups of TMP are electronically very similar to the phenyl groups of TPP. The most interesting piece of information derived from Figure 5 is that upon fusing the neocuproine

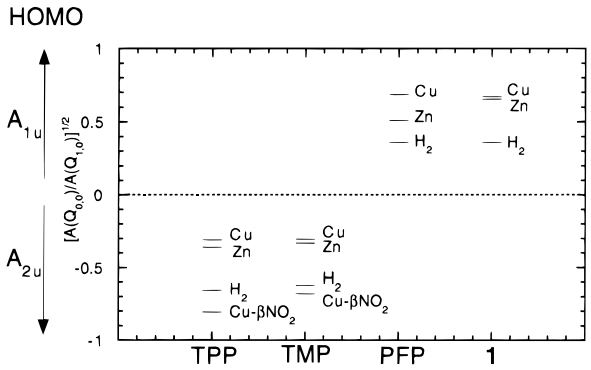

Figure 5. Energy differences between the a_{1u} and a_{2u} orbitals in the indicated porphyrins based on the Q-band ratios shown in Table 2.

moiety onto the β-positions of the TMP core there is an inversion in the nature of the HOMO. This assignment is based on the observed trend in the ratio of the Q-band absorbance values upon metalation. The orbital most affected by metalation is the b_1 orbital, which has considerable electron density at the pyrrole nitrogens (Figure 4). The electron-withdrawing metal ion has a stabilizing effect on this orbital. Therefore, when the HOMO is the b_1 orbital, metalation reduces the energy gap between the b_1 and b_2 orbitals, resulting in a smaller value for the ratio of the Q-band absorbance values when compared to those of the free-base porphyrin. This trend is indeed observed within the TMP and TPP compounds, which are known to have the b_1 orbital as the HOMO. Thus, the values of $A[\mathrm{Q}(0,0)]/A[\mathrm{Q}(1,0)]\}^{1/2}$ are negative for those compounds with an a_{2u} (b_1) HOMO, as can be seen by eq 1. If, however, the b_2 orbital is the HOMO, then metalation would increase the energy gap between the two top-filled orbitals, resulting in an increase in the value of the ratio of the Q-band absorbance values. The PFP compounds, which are known to have the b_2 orbital as the HOMO, show this trend.[11,22] Compounds H_2**1**, Zn**1**, and Cu**1** have a b_2 HOMO on the basis of the fact that the ratio of the Q bands increases in the order H_2**1** < Zn**1** < Cu**1** (Figure 5). Determination of the HOMO structure is important if one wishes to study energy- and electron-transfer involving such complexes. Since we plan to study energy and electron transfer between chromophores linked through the fused neocuproine unit, a b_2 HOMO is desirable to maximize the rates of such processes.

(d) B-Band Analysis of $H_2$1, Cu1, and Zn1. The B-band structure of H_2**1**, Cu**1**, and Zn**1** is dramatically different from those of the parent porphyrin, H_2TMP, and its copper(II) and zinc(II) complexes (see the Supporting Information). The observed broadening of the B band has been attributed to the extension of the π-system of the porphyrin into the neocuproine portion of the molecule.[21] The full width at half-maximum (fwhm) values are 1808, 3730, and 3433 cm^{-1} for H_2**1**, Cu**1**, and Zn**1**, respectively, while the fwhm values for H_2TMP, CuTMP, and ZnTMP are 687, 521, and 622 cm^{-1}, respectively. The B-band envelope of the metallo complexes, Cu**1** and Zn**1**, is considerably different from that of H_2**1**, in that it is split into two relatively sharp transitions (Figure 3). Excitonic coupling is precluded as a possible explanation since it has been established that good electronic communication exists between the porphyrin and neocuproine substituents.[21,35] A more plausible explanation would be to describe the two transitions as the B_x and B_y transitions of the molecule. The x and y molecular dipole axes lie along the two planes containing opposite pyrrole

(35) Kasha, M.; Rawls, H. R.; El-Bayoumi, M. A. *Pure Appl. Chem.* **1965**, *11*, 371−392.

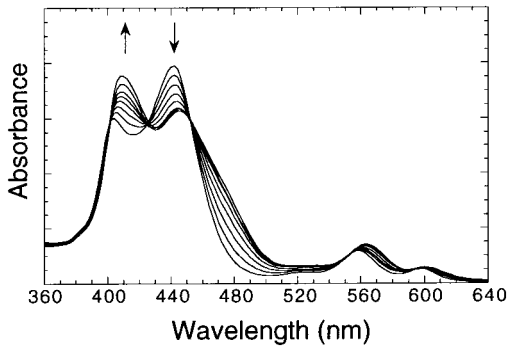

Figure 6. Overlay of absorption spectra in CH_3CN at room temperature for Cu**1** with 0, 0.17, 0.25, 0.33, 0.41, 0.50, 0.83, and 1.2 equiv of $[Cu(CH_3CN)_4](PF_6)$. Initial [Cu**1**] = 6.36×10^{-6} M. All spectra were corrected for changes in concentration due to the addition of copper(I).

nitrogens. For purposes of this discussion, we will assign the *y*-axis as that containing the pyrrole fused to the neocuproine subunit. If we invoke this formalism, then it becomes obvious that the two transition dipoles are no longer equivalent in our molecules. Furthermore, we can now assign the high-energy band as the B_y transition and the lower energy band as the B_x transition.[33,34]

A similar splitting in the B band is observed in the reduced zinc porphyrin molecule, zinc hexahydroporphyrin, in which three pyrrole rings are reduced at the β positions.[33] This molecule has C_{2v} symmetry, like the metallo compounds Cu**1** and Zn**1**. Therefore, the molecular symmetry of these porphyrins may contribute to the splitting of the B bands.

(III) "External" Metal Binding. (a) Titrations in Acetonitrile. Various metal salts have been titrated into acetonitrile solutions of Cu**1** to determine if there is a spectral dependence on the nature of the metal ion coordinated "externally" to the neocuproine moiety. The results of a typical spectrophotometric titration can be seen in Figure 6, where $[Cu(CH_3CN)_4](PF_6)$ was the metal ion source added. Other metal salts used include $LiBF_4$, $Zn(BF_4)_2$, $Ni(BF_4)_2$, and $Cu(BF_4)_2$. All of these metal ions form bis(chelate) complexes with neocuproine.[36] All of the spectrophotometric titrations gave the same general results, with only small variations in the extent to which the B_y and B_x bands shifted. The general spectroscopic changes observed are a red shift of all peaks, a reduction in the intensity of the B_x band, an increase in the intensity of the B_y band, and a general broadening of the B band (Figure 6). It is clear from these results that the B state in Cu**1** is extremely sensitive to external metal ion coordination. Also, the absorption spectrum of Cu**1** is much more sensitive to external metal binding than that of the previously studied free-base porphyrin, H_2**1**.[21]

The spectral changes that occur upon binding of metal ions to the neocuproine moiety of Cu**1** are believed to be electrostatic in nature, since excitonic theory predicts that the B_x band should blue shift, while the B_y band is predicted to shift to the red.[3,35] Also, excitonic theory does not predict the observed dramatic changes in intensities of the B_x and B_y bands.[3,35]

Although the shifts and intensity changes in the spectra were insensitive to the nature of the metal ion titrated, the rates at which spectroscopic changes were observable did vary slightly. Zinc(II) and both copper(I) and copper(II) ions resulted in instantaneous changes in the spectra even upon addition of 0.1 equiv of the metal ion. Nickel(II), however, required a longer stirring period before changes were observable in the absorption spectra. When lithium(I) was titrated into an acetonitrile solution of Cu**1**, there were no spectral changes even upon addition of up to 100 equiv of Li^+. However, when the titration was performed in methylene chloride, lithium behaved much like the zinc and copper ions. These results suggest that the binding constant for lithium and the neocuproine moiety is significantly lower in acetonitrile than in methylene chloride.

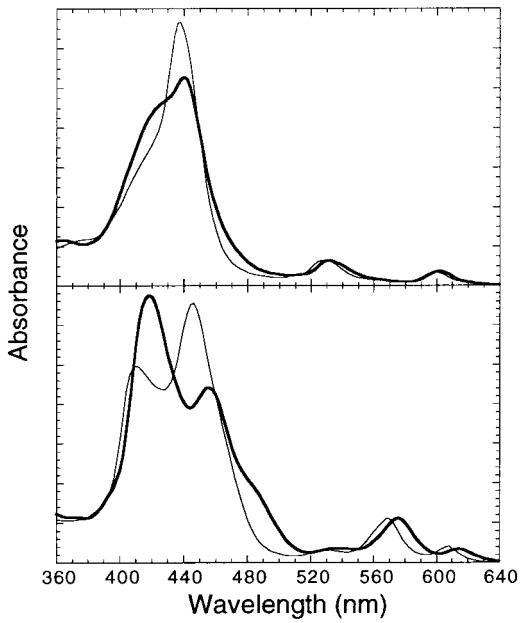

Figure 7. Absorption spectra in CH_2Cl_2 at room temperature for (top) H_2**1** (thin line) and $[Zn(H_2\mathbf{1})_2](CH_3CO_2)_2$ (thick line) and (bottom) Zn**1** (thin line) and $[Zn(Zn\mathbf{1})_2](CH_3CO_2)_2$ (thick line).

An additional experiment was performed to test the stability of the metal−neocuproine complexes in acetonitrile. A solution containing 4 equiv of Zn^{2+}/equiv of Cu**1** was diluted, and spectra were taken over time. It was observed that the spectra slowly reverted to an "intermediate spectrum", similar to one in which fewer equivalents of metal ion were added. Further dilution resulted in a spectrum very similar to that of Cu**1**. Thus, the concentration dependence of the spectra demonstrate that dissociation is likely occurring, and that, at low concentrations, there is likely a mixture of Cu**1**, $[Zn(Cu\mathbf{1})]^{2+}$, and $[Zn(Cu\mathbf{1})_2]^{2+}$ in acetonitrile.

(b) Examination of the Zinc Bis(porphyrin) Complex, $[Zn(Zn\mathbf{1})_2]^{2+}$. Since we were interested in directly probing the spectral differences between the metallo derivatives of **1** and the bis(porphyrin) $[M(M\mathbf{1})_2]^{n+}$ complexes, we examined the spectra of the complex $[Zn(Zn\mathbf{1})_2]^{2+}$ in methylene chloride. Mass spectrometry and ^1H NMR data confirm that, in methylene chloride, this complex is stable as the bis(chelate), without dissociation to $[Zn(Zn\mathbf{1})]^{2+}$.[37] In addition, the spectrum of $[Zn(Zn\mathbf{1})_2]^{2+}$ is invariant over the concentration range of 1×10^{-5} to 1×10^{-6} M, allowing us to compare both the absorption and emission properties with those of the previously reported complex $[Zn(H_2\mathbf{1})_2]^{2+}$.[21] Figure 7 shows the absorption spectra of Zn**1** and H_2**1** and their Zn^{2+} complexes. The changes in the spectrum of Zn**1** induced by external metal binding are practically identical to those observed in the titrations of Cu**1** with the different metal ions (Figure 6). This is not surprising since the Q-band ratios for Cu**1** and Zn**1** (Figure 5) are nearly identical. Zn**1** is spectroscopically much more sensitive to external metal binding than H_2**1**, not only because of the observed dramatic changes in the B band, but also because the

(36) Gantzel, P. K.; Vannelli, T. A.; Joshi, H. S.; Guidolin, M.; Karpishin, T. B. Manuscript in preparation.

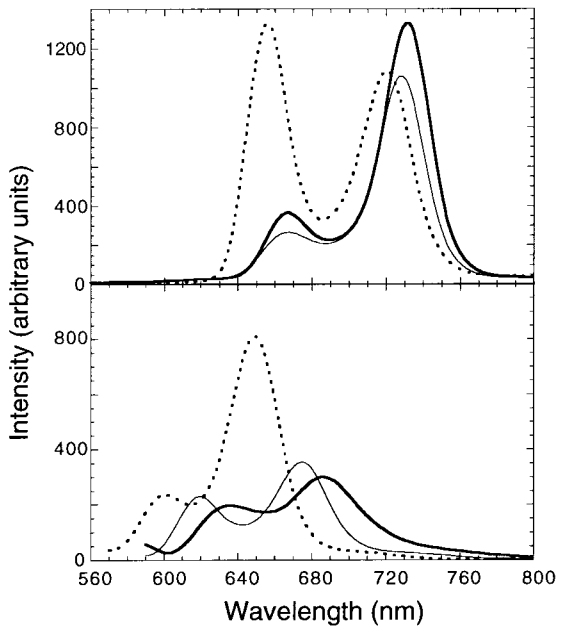

Figure 8. Corrected emission spectra in CH_2Cl_2 at room temperature for (top) H_2TMP (λ_{ex} = 514 nm) (dashes), H_2**1** (λ_{ex} = 528 nm) (thin line), and $[Zn(H_2\mathbf{1})_2](CH_3CO_2)_2$ (λ_{ex} = 532 nm) (thick line) and (bottom) ZnTMP (λ_{ex} = 550 nm) (dashes), Zn**1** (λ_{ex} = 568 nm) (thin line), and $[Zn(Zn\mathbf{1})_2](CH_3CO_2)_2$ (λ_{ex} = 576 nm) (thick line). All spectra were normalized to identical OD values at the excitation wavelength.

bands shift to the red more than those in the free-base system. The B_y and B_x bands of Zn**1** shift by 348 and 492 cm^{-1} while the B band of H_2**1** only shifts by 104 cm^{-1} upon complex formation with zinc(II). The Q(1,0) band in Zn**1** shifts to the red by 244 cm^{-1} in comparison to 21 and 11 cm^{-1}, respectively, for the Q_y(1,0) and Q_x(1,0) bands of H_2**1**. Another interesting difference between the two complexes is that $[Zn(Zn\mathbf{1})_2]^{2+}$ has a shoulder on the low-energy side of the B band, while the analogous free-base compound lacks this feature (Figure 7).

(IV) Emission Spectra. Figure 8 shows the corrected Q-band emission spectra of H_2**1**, Zn**1**, and the Zn^{2+} complexes, $[Zn(H_2\mathbf{1})_2]^{2+}$ and $[Zn(Zn\mathbf{1})_2]^{2+}$. The corrected spectra for H_2TMP and ZnTMP are provided for comparison. Note that, as a general trend, the emission intensities for the zinc porphyrins are lower than those of the free-base porphyrins. The higher energy emission band is due to the Q(0,0) transition, i.e., from the lowest vibrational mode of the excited state to the lowest vibrational mode of the ground state. The lower energy band is assigned as Q(0,1), which arises from relaxation of the excited electron to the first vibrational mode of the ground state.[33] The general trends observed in the absorption spectra among ZnTMP, Zn**1**, and $[Zn(Zn\mathbf{1})_2]^{2+}$ are also observable in the emission spectra. There is a red shift of 497 cm^{-1} in the Q(0,0) emission band between ZnTMP and Zn**1** and 419 cm^{-1} between Zn**1** and $[Zn(Zn\mathbf{1})_2]^{2+}$, while the Q(0,1) transition shifts by 593 and 259 cm^{-1}, respectively. When H_2**1** is compared to its zinc(II) complex, these shifts are much smaller: 23 and 48 cm^{-1} for the Q(0,0) and Q(0,1) transitions, respectively. The integrated intensities vary little between Zn**1** and its zinc(II) complex, 60% and 64%, respectively (ZnTMP = 100%). This increase in intensity upon complex formation with zinc(II) is also observed in the free-base system, but to a greater extent; the emission spectrum of the zinc(II) complex of H_2**1** is 25% more intense than that of H_2**1**. It can also be seen in Figure 8 that the emission bands of $[Zn(Zn\mathbf{1})_2]^{2+}$ are broader than those of Zn**1**, and that, relative to ZnTMP, for both Zn**1** and $[Zn(Zn\mathbf{1})_2]^{2+}$ the Q(0,0) emission band increases in intensity relative to the Q(0,1) band. These emission data, combined with the absorption data, provide compelling evidence that the binding of a closed shell metal ion (Zn^{2+}) to the neocuproine unit of Zn**1** elicits significant changes in the electronic structure of the chromophore.

Conclusions

Notable differences in the B-band region are observed between H_2**1** and its metal complexes, Cu**1** and Zn**1**. From analysis of absorption and emission spectra, these metalloporphyrins also display an increased spectroscopic sensitivity to external metal ion binding relative to H_2**1**. Interestingly, the absorption spectra of Cu**1** and Zn**1** are insensitive to the nature of the metal ion bound externally. Assignment of the b_2 orbital as the top-filled porphyrin π orbital (HOMO) in compounds H_2**1**, Cu**1**, and Zn**1** was achieved using a spectroscopic technique based on Gouterman's four-orbital model. Although the HOMO is the same in all three compounds, the energy gap between the two HOMOs is greater for Cu**1** and Zn**1** than it is for H_2**1**. This difference in the HOMO energy levels likely contributes to the observed spectroscopic differences between H_2**1** and the metallo derivatives, Cu**1** and Zn**1**.

Since the molecules under study possess a b_2 HOMO, which has substantial electron density at the β-pyrrole positions (Figure 4), these compounds are excellent candidates as building blocks for multiporphyrin systems with a high degree of electronic communication between the chromophores. Thus, having now characterized the HOMO of these novel chromophores, future work is planned to examine bis(porphyrin) complexes with two different porphyrins, utilizing methods recently developed for making heteroleptic bis(phenathroline) complexes.[38]

Acknowledgment. We thank Professor Y. Tor for the use of his emission spectrometer. This research was supported by the NIH (training grant to T.A.V.) and by a Hellman Faculty Fellowship (to T.B.K.).

Supporting Information Available: Absorption spectra of H_2TMP, CuTMP, and ZnTMP. This material is available free of charge via the Internet at http://pubs.acs.org.

IC990914Q

(37) ^{1}H NMR titrations of $Zn(CH_3COO)_2\cdot 2H_2O$ into Zn**1** were performed in $CDCl_3$. As various amounts of Zn^{2+} ion were added, all three of the porphyrin species, Zn**1**, $[Zn(Zn\mathbf{1})(CH_3COO)_2]$, and $[Zn(Zn\mathbf{1})_2]^{2+}$, could be observed by examination of the chemical shifts of the phenanthroline methyl groups. This information allows for unambiguous identification of $[Zn(Zn\mathbf{1})_2]^{2+}$ as the only species in $CDCl_3$ when the complex is prepared as described in the Experimental Section.

(38) Miller, M. T.; Gantzel, P. K.; Karpishin, T. B. *J. Am. Chem. Soc.* **1999**, *121*, 4292−4293.